MEMOIRS OF THE COLLEGE OF SCIENCE, UNIVERSITY OF KYOTO, SERIES B,
Vol. XXVIII, No. 4 Geology and Mineralogy, Article 3, 1962

Role of Pyrrhotite in Rock Magnetism

By

Yong-ho KANG

Geological and Mineralogical Institute, University of Kyoto

(Received November 1, 1961)

Abstract

Natural occurrence of pyrrhotite in iron-sulfide mines in Japan was described in part 1 of this paper, together with the experimental results of synthesis of the mineral under high pressure and temperature. While in the second part are mentioned the mechanism in the acquisition of the remanent magnetism of rocks containing pyrrhotite, and several demagnetizing experiments to make palaeomagnetic interpretation.

Introduction

The chemical composition of pyrrhotite is represented by the formula FeS_{1+x} ($0<x<0.20$), and the crystallographic structure belongs to dihexagonal group[1]. Its magnetic properties have been studied on both sides of theory and experiment[2,3], showing that pyrrhotite is basically antiferromagnetic material accompanied by weak ferromagnetism, although some of the properties change with change of the value x in FeS_{1+x}.

Regarding the natural occurrence, there are many studies[4,5,6] reporting the precise origin, formation or occurrence of this mineral, but there have been a few reports in which the author argued the significance of pyrrhotite in rock magnetism. Recently, Kawai and the present author[7] discovered many Japanese sedimentary rocks of Mesozoic and Palaeozoic ages in which pyrrhotite is the host ferromagnetic mineral and responsible for the magnetization of these rocks.

In this paper the present author will show occurrences of pyrrhotite in iron-sulfide mines and in sedimentary rocks in Japan, together with the results of magnetic properties of synthesized pyrrhotites, and also discuss the contribution of the mineral to rock magnetism.

Chapter 1. Pyrrhotite Occurring in Iron-Sulfide Ore-deposits

107 rock samples were collected from two representative iron-sulfide mines in Japan, Besshi Mine of Ehimi Prefecture and Yanahara Mine of Okayama Prefecture. The collecting sites are shown in Fig. 1.

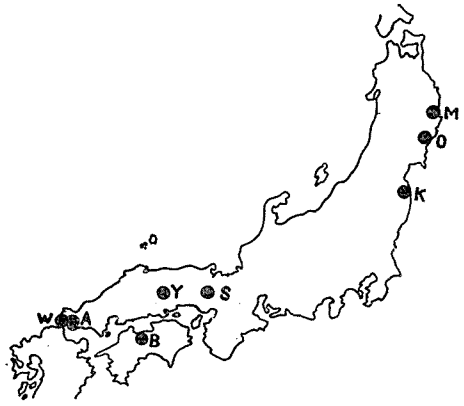

Fig. 1. Distribution of the collecting sites. Samples of iron-sulfide ore-deposits were collected from the places B and Y, red sandstones from S, A and W, and black shales from W, M, O and K.
B: Besshi ore-deposit (Ehime Prefecture), Y: Yanahara ore-deposit (Okayama Prefecture), S: Sasayama (Hyôgo Prefecture), A: Asa (Yamaguchi Prefecture), W: Yoshimi (Yamaguchi Prefecture), M: Miyako (Iwate Prefecture), O: Ôfunato (Iwate Prefecture), K: Kashima (Fukushima Prefecture).

1. Measurements of remanent and saturation magnetization

a) *Rocks from Besshi ore-deposit*

First, rocks were collected from several places in one ore-deposit with different altitudes from sea level and next, the same way of the collection was applied on several ore-deposits to trace a relationship between the shapes of ore deposits and their magnetization.

The rocks thus obtained were iron-sulfide ores, country rocks of crystalline schist and rocks from the contact zone of ore-deposits and schists.

The measurements of the natural remanent magnetization (n.r.m.) were made by means of an astatic magnetometer[8] and the thermo-magnetic analyses by a Sucksmith type thermo-magnetic balance[9]. The summarized results shown in Figs. 3 and 4, and in Table I indicate that the magnetization of these rocks is very strong and stable, and also there is a remarkable difference in the direction of the n.r.m. between the upper part and the lower part of the deposit. The mean direction of magnetization is about NE 15° in declination and 45° down in inclination in the upper part, while that of the lower part is about NW 31° and 53° down respectively.

This deposit which belongs to Sambagawa metamorphic zone has been produced by a regional dynamo-metamorphism and consists of various kinds of crystalline schists. In order to examine the relation between the structure of the deposit and the direction of the magnetization, a vertical section of the

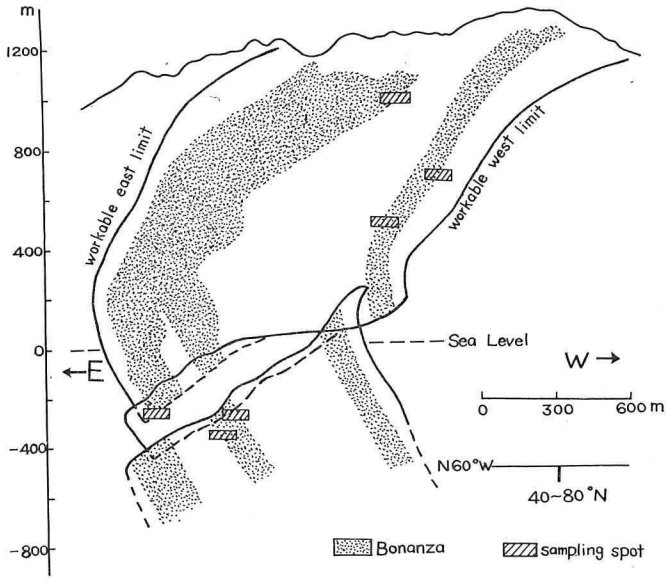

Fig. 2. Sampling spots in Besshi ore-deposit.

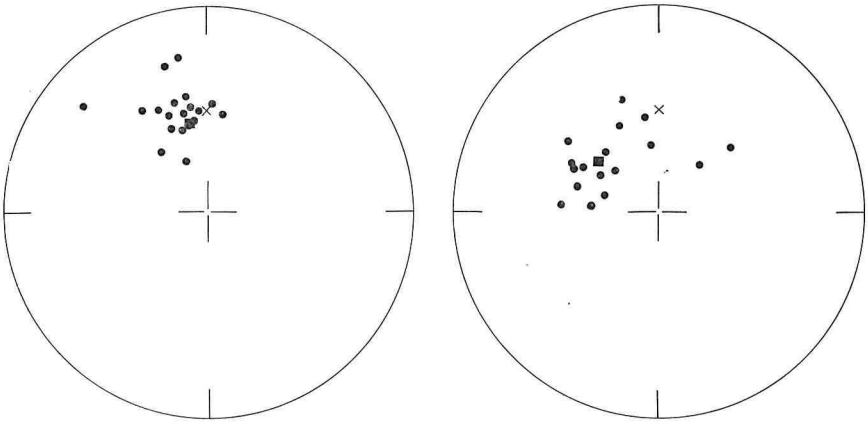

(a) for rocks collected at 350 m below sea level

(b) for rocks collected at 260 m below sea level

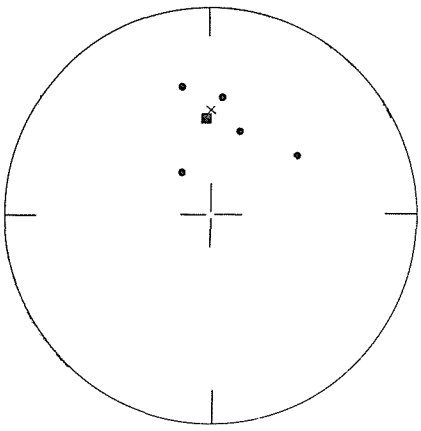

(c) for rocks collected at 480 m above sea level

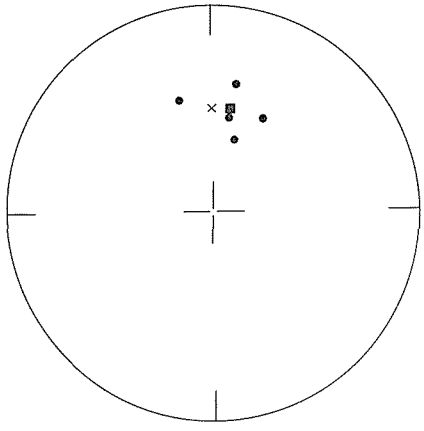

(d) for rocks collected at 660 m above sea level

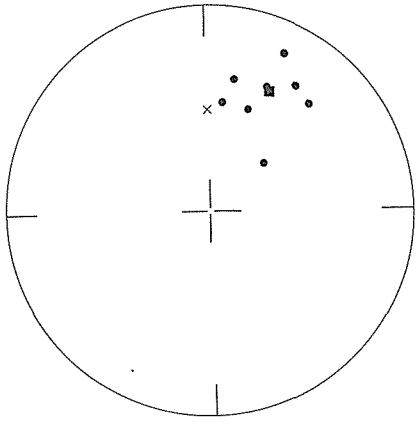

(e) for rocks collected at 975 m above sea level

Fig. 3. Direction of the n.r.m. of rocks plotted on the Schmidt's equal areal projection. Circles represent the direction of north poles on lower hemisphere.

× : Direction of the present dipole field

▩ : Mean direction of the n.r.m.

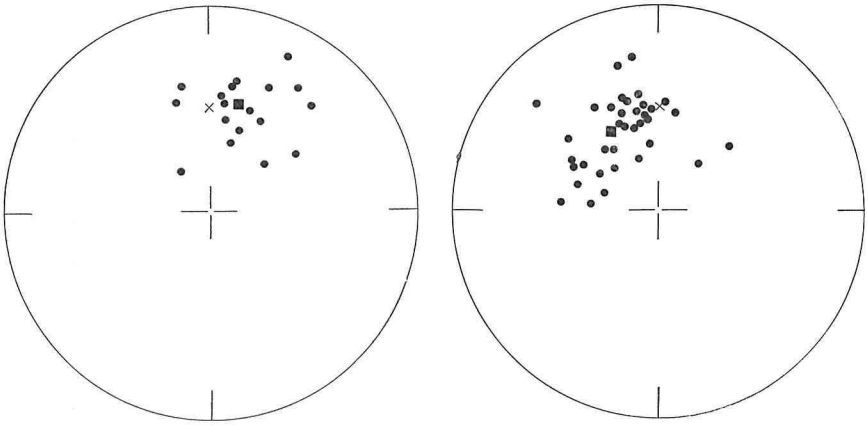

(a) Upper part (above sea level) (b) Lower part (below sea level)

Fig. 4. Direction of the natural remanent magnetization of upper part and lower part of the ore-deposit. ×: Direction of the present dipole field, ■: Mean direction of the n.r.m..

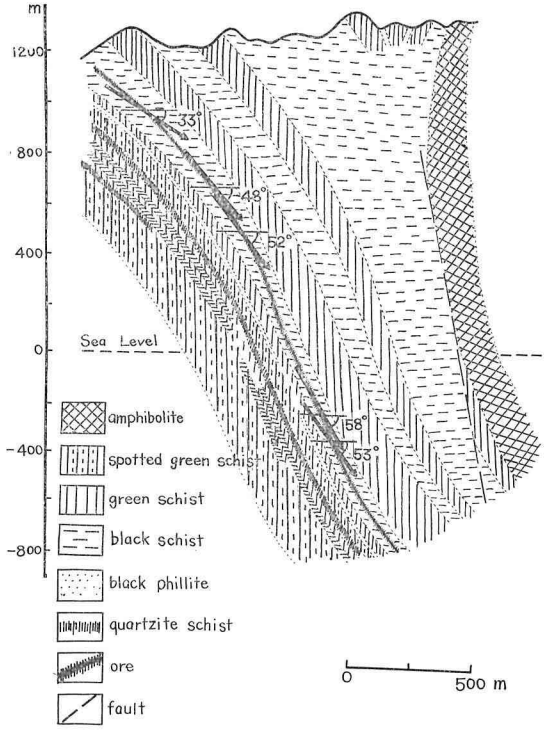

Fig. 5. Relation between the direction of magnetization and the inclination of the ore-deposit.

Table I

No.	Sampling level	Rock	Direction of Magnetization		Jr $\left(\times 10^{-3}\frac{emu}{g}\right)$	Ji $\left(\times 10^{-3}\frac{emu}{g}\right)$	Js $\left(\times 10^{-1}\frac{emu}{g}\right)$	Curie point (°C)
			Decl.	Incl.				
1	−350 m	quartz						
2		ore	NW 17°	55°D	0.78	0.27	3.51	300
3		ore & q.	13	49	0.24	0.02	1.41	300
4		ore	8	53	0.25	0.09	2.00	310 570
5		quartz						
6		ore & q.	5	49	0.36	0.02	2.14	320
7		ore & q.	8	42	1.34	0.17	6.86	305 570
8		ore	12	54	1.86	0.38	11.35	290
9		ore	9	47	1.08	0.25	9.43	295
10		ore	− 3	46	1.75	0.40	26.04	295
11		green	37	59	0.05	0.01	0.48	280 550
12		ore						
13		quartz	22	68	0.07	0.01	2.42	300
14		green						
15		green	23	53	0.29	0.03	7.81	295
16		green						
17		green						
18		quartz					para.	
19		ore	17	43	2.12	0.76	26.06	305 565
20		ore						
21		graphite						
22		graphite						
23		green & o.	25	43	0.68	0.65	1.40	300
24		ore & q.	32	40	1.62			
25		ore & q.	−10	50	0.16	0.02		
26		green	21	48	0.02			
27		green						280
28		ore					para.	
29		ore					para.	
30	−260 m	ore & q.	86	51	0.17	0.06	0.30	300
31		ore	7	63	0.03	0.01	8.80	295
32		ore	47	66	0.29	0.11		
33		graphite					para.	
34		quartz					para.	
35		quartz					para.	
36		ore	73	56	1.73	0.35	21.95	295
37		ore & q.	61	50	0.95	0.39	7.81	295
38		ore	60	55	0.68	0.10	6.14	295
39		o. & green	44	58	3.30	0.85	37.20	310 575
40		graphite	58	62	0.14	0.07	0.53	270 575
41		ore						300 660

Table I (Continued)

No.	Sampling level	Rock	Direction of Magnetization		Jr ($\times 10^{-3}$ emu/g)	Ji ($\times 10^{-3}$ emu/g)	Js ($\times 10^{-1}$ emu/g)	Curie point (°C)
			Decl.	Incl.				
42		o. & green	NW 52°	43°D	14.90	4.80		300 580
43		green						
44		o. & green	85	63	1.30	0.30		285 575
45		o. & green	73	68	331.81	298.62		
46		ore & q.	63	52	339.84	234.52		575
47		ore	25	52	1.61	0.49	0.87	300
48		graphite						300 575
49		ore & q.	9	51	12.36	2.43	1.52	
50		ore	19	42	1.01	0.63	3.97	
57	+480 m	quartz						
58		green						
59		ore	34	69	43.47	153.61		580
60		quartz						
61		quartz						
62		ore	− 5	42	498.58	478.65		275 570
63		quartz	−18	55	6.88	3.84		
64		ore	−55	48		62.80		
65		ore						
66		ore & q.	13	37	2.63	0.03		580
67	+660 m	ore	−10	39	45.34	39.42		
68		ore	−28	47	406.47	321.09	26.70	280 575
69		quartz					para.	
70		green						
71		piedmontite	15	43			1.46	
72		ore & q.	−15	59	0.50	0.71		300 670
73		green						
74		quartz						
75		green & o.	− 9	51	288.64	251.05		310 570
76		green						
77	+975 m	green					para.	
78		ore & q.	−36	26	2.81	0.60		
79		ore & q.	−43	29	266.03	274.04		
80		ore					para.	
81		green					para.	
82		green					para.	
83		ore & q.	− 9	45	191.44	313.92		
84		quartz						
85		ore & q.	−27	15	968.90	121.10		575
86		ore & q.	−27	34	427.91	380.80		575
87		ore & q.	−13	36	2.63	0.70	0.42	300 575
88		quartz	−21	45	0.40	0.41	0.30	275 575

deposits and their surrounding area is drawn in Fig. 5. In this diagram the direction of the n.r.m. of rocks were plotted at the spots where they were collected. As can be observed in the figure, the direction of the n.r.m. is nearly parallel to the general trend of the ore-deposit.

The special remarks should be given to the following facts: (1) The intensity of magnetization of the ore and the country rocks is too weak to be measured but that of rocks from the contact zone is fairly strong, the order of the intensity being $n \times 10^{-4}$ e.m.u./g in average. As will be mentioned later, this differs greatly from the case of Yanahara Mine. (2) There exists a noticeable correlation between the direction of the magnetization and the bending structure at the central part of the deposit, that is, the direction of the n.r.m. is almost parallel to the average direction of each ore-deposit as seen in Figs. 2 and 6.

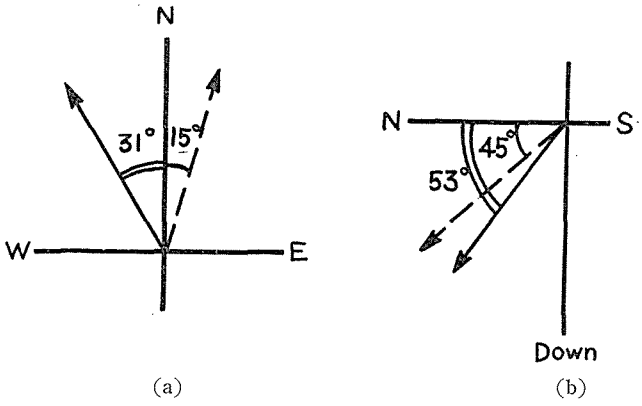

Fig. 6. Schematic representation of the n.r.m. of Besshi mine. Full lines show the direction of the lower part and dotted lines that of the upper part. (a) Declination (b) Inclination.

Next the thermo-magnetic analyses of the rocks were carried out. The intensity of saturation magnetization and the Curie points are measured on nearly all of the samples. As seen in the results, (Fig. 7 and Table I), the rocks contain three kinds of ferromagnetic minerals and they are considered to be FeS_{1+x}, Fe_3O_4 and α-Fe_2O_3, because their Curie points are 300°C, 580°C and 670°C respectively and correspond to the above-mentioned three minerals. It is also observed that magnetite and haematite are more predominant ferromagnetic minerals than FeS_{1+x} in the upper part of the deposit, but the other way in the lower, and the intensity of the magnetization in the lower is much weaker than that in the upper.

The existence of these FeS_{1+x}, Fe_3O_4 and α-Fe_2O_3 can be observed even by naked eye.

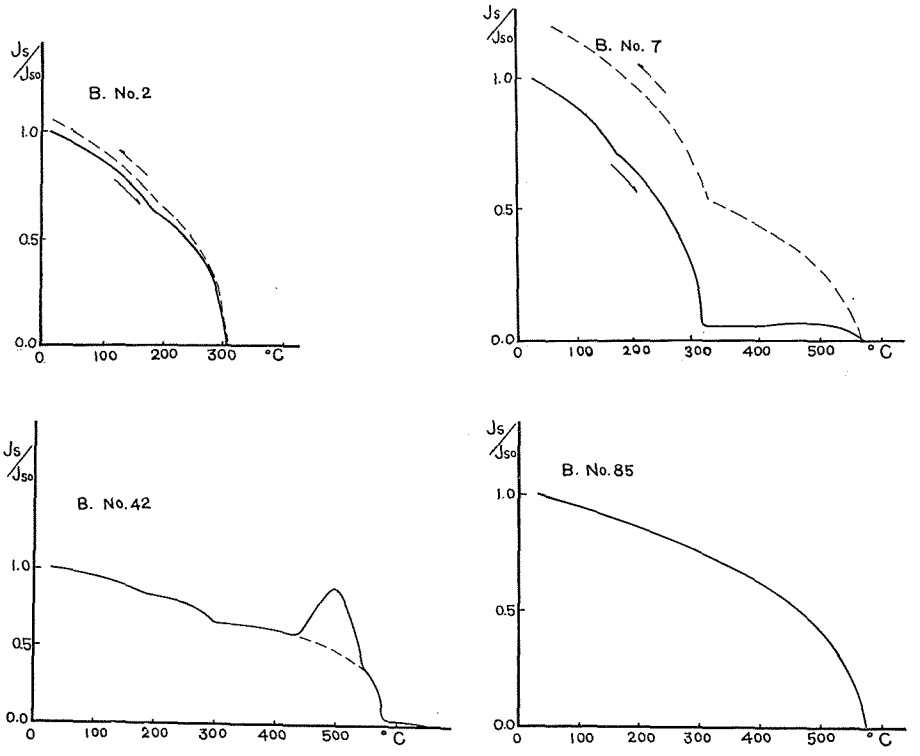

Fig. 7. Some examples of thermo-magnetic analyses of rocks from Besshi ore-deposit.

b) *Magnetization of Yanahara ore-deposit*

KATO mentioned in his precise study on Yanahara Mine[10] that the origin of the formation of this deposit is due to the igneous activities. In order to compare the magnetization of this deposit with that of Besshi, rock samples were collected, and the measurements of the n.r.m. and the thermo-magnetic analyses were carried out. These results are shown in Figs. 8 and 9, and in Table II.

The rocks possess fairly strong n.r.m. in both of the deposit and the country rock, the average direction

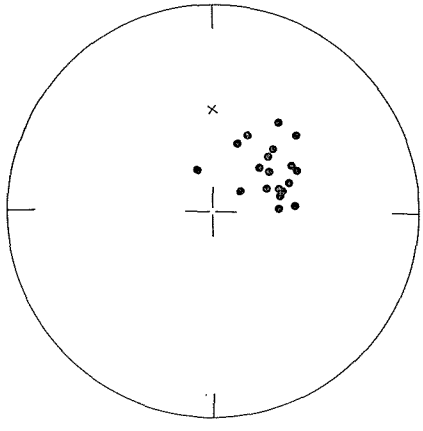

Fig. 8. Direction of the n.r.m. of Yanahara ore-deposit.
× : Direction of the present dipole field.

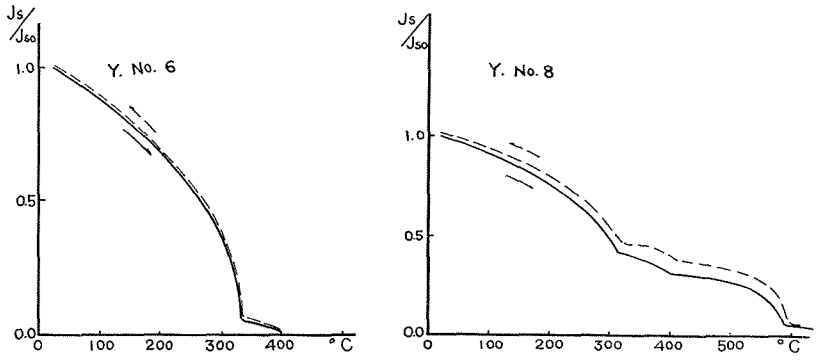

Fig. 9. Some examples of thermo-magnetic analyses of rocks from Yanahara ore-deposit.

Table II

No.	Rock	Direction of Magnetization		Jr $\left(\times 10^{-3}\frac{\text{emu}}{\text{g}}\right)$	Ji $\left(\times 10^{-4}\frac{\text{emu}}{\text{g}}\right)$	Js $\left(\times 10^{-1}\frac{\text{emu}}{\text{g}}\right)$	Curie point (°C)
		Decl.	Incl.				
1	diabase	NE 43°	55°D	0.42	0.67	0.74	330
2	porphyrite	63	53	0.14	0.20	2.56	330 400
3	diabase	35	47	0.76	0.53		
4	ore	76	62	4.00	8.40	58.60	310
5	ore	51	77	1.48	3.11	67.10	320
6	ore	46	64	0.71	0.71	6.52	330 400
7	ore	89	64	0.74	0.59	4.34	330
8	porphyrite	75	62	0.23	0.12	0.41	315 400 580
9	ore	86	57	0.90	0.72		
10	diabase	69	57	0.05	0.05	0.15	320
11	ore	47	44	0.57	0.68	3.62	335
12	diabase	53	62	0.69	1.24	1.01	315
13	ore	66	67	2.13	1.49	116.30	315
14	porphyrite	44	59	0.41	0.37	0.68	330
15	ore	−23	71	1.04	0.73	16.01	315
16	ore	57	53	0.40	0.76	2.74	330
17	ore	19	61	1.25	2.13	70.23	320
18	diabase	23	56	0.16	0.05	0.06	315
19	diabase	72	62	1.98	4.95	2.97	320

being NE 54° in declination and 62° down in inclination. Roughly speaking, the direction of the magnetization of the deposit appears parallel to that of the country rock, and the saturation magnetization due to FeS_{1+x} is stronger than that of Besshi deposit, suggesting that the mechanism of the formation of the mine differs from that of Besshi.

2. Synthesis of FeS_{1+x}

Néel pointed out that the spontaneous magnetization of FeS_{1+x} is due to the ordered arrangement of vacancies of iron ions in the crystal[2], and the magnetic properties of FeS_{1+x} change with the amount of sulfur atoms therein[3,11,12,13]. The author made a synthesis of FeS_{1+x} under the atmospheric and the high pressure to investigate the relations between its chemical composition, the magnetic properties and the crystallographic structure.

a) *Synthesis of FeS_{1+x} under one atmospheric pressure*

Pyrrhotite was synthesized by exposing H_2S gas on iron in air at high temperatures. This method can be represented by the following chemical equation.

$$Fe + H_2S \xrightarrow[400°C-1{,}000°C]{1\,atm} FeS_{1+x} + (FeS_2) + H_2\uparrow$$

Fig. 10 shows the relation between the heating temperatures and the chemical composition of pyrrhotite in equilibrium at each temperature. As seen in the figure, at temperature below 650°C, pyrrhotite with the composition of (Fe/S $\approx$1/1.15) was formed in coexistence with pyrite. Above this temperature, however, the ratio of sulfur to iron tends to decrease with the increase of temperature and finally $FeS_{1.06}$ can be formed at about 1,000°C.

The composition of synthesized pyrrhotite was determined by measuring the weight change of specimens to occur when they were calcined to α-Fe_2O_3. Next, X-ray analyses were made to correlate the chemical composition to the lattice costant (Fig. 11). In the results of the thermo-magnetic analyses (Figs. 12 and 13), it was found that the intensity of the saturation magnetization and the Curie point change remarkably with the change of their compositions.

b) *Synthesis of FeS_{1+x} under high pressures*

Several runs of experiment were done, using the following three kinds of specimens for the purpose of studying a certain condition of temperature and pressure under which pyrrhotite has been formed from pyrite because the chemical change of pyrite to pyrrhotite would take place in the existence of high pressures. The starting materials are (1) dry FeS_2 powders, (2) wet FeS_2 powders containing water and (3) the mixture of Fe and S powders. In the case of the dry FeS_2, no change was found under applied pressures up to 20,000 kg/cm^2 at 350°C. However, as for the wet FeS_2, the production of FeS_{1+x} was detected in the results of the thermo-magnetic analysis as shown

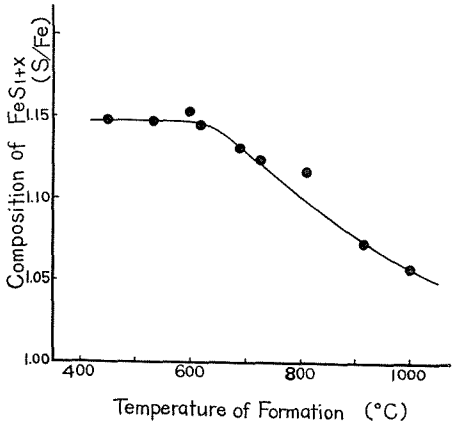

Fig. 10. Relationship between the chemical composition and the heating temperature on the synthesis of pyrrhotite.

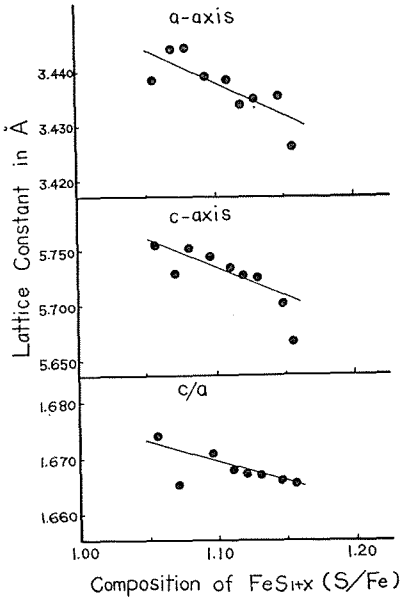

Fig. 11. Relationship between the chemical composition and the lattice constant of the synthesized pyrrhotite.

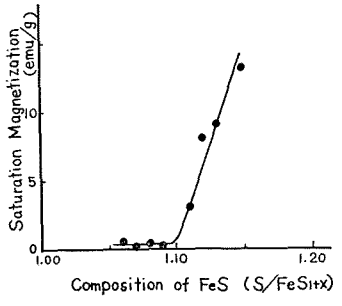

Fig. 12. Relationship between the intensity of the saturation magnetization and the chemical composition of synthesized pyrrhotite.

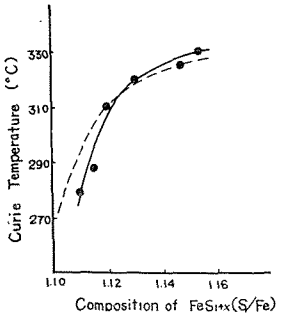

Fig. 13. Relationship between Curie temperature and the chemical composition of synthesized FeS_{1+x}. Dotted line shows the result obtained by Haraldsen (1937).

in Fig. 14. The schematic chemical equation of this reaction is represented in the following way.

$$FeS_2 \xrightarrow[(H_2O),\ 350°C]{3{,}500\text{–}8{,}000\ kg/cm^2} FeS_{1+x} + (1-x)S$$

Next, the same experiment was attempted with mixture of iron and sulfur.

$$Fe + S \xrightarrow[200°C]{3{,}300\text{–}7{,}000\ kg/cm^2} FeS_{1+x}$$

When pressure which is less than 3,300 kg/cm² or more 7,000 kg/cm² was applied to the specimen at about 200°C, no change was detected, but in the range from 3,300 to 7,000 kg/cm² the production of FeS_{1+x} was confirmed as seen in Fig. 15. The range of pressures under which pyrrhotite

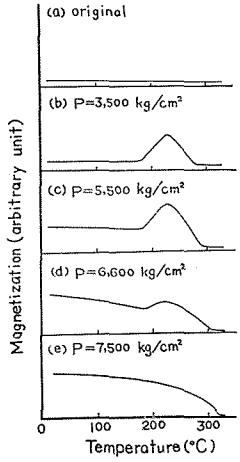

Fig. 14. Temperature dependency of the magnetization of pyrrhotite synthesized by heating pyrite powders at 350°C under one-directional pressure.

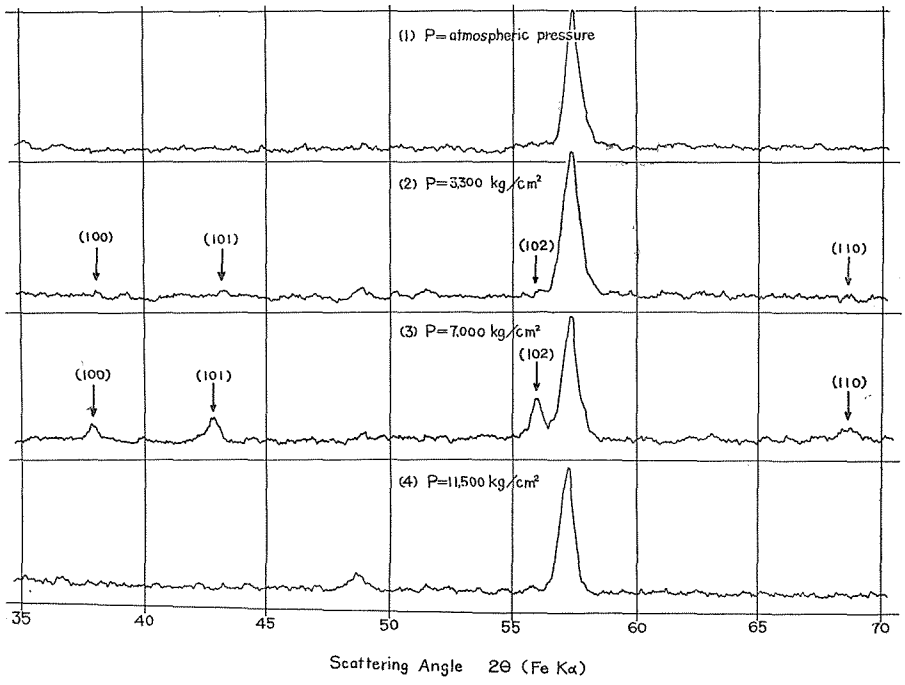

Fig. 15. X-ray diffraction patterns of pyrrhotite made by heating the mixture of iron and sulfur powders at 200°C under one-directional pressure.

is synthesized in this case is nearly same as that under which the wet pyrite convert to pyrrhotite.

3. The effect of pressures on the magnetic properties of FeS_{1+x}

Recently, many works have been carried out on the effect of pressures upon the magnetic properties of haematite, magnetite and other ferrimagnetic minerals in rocks[14,15,16,17] except the influence of pressures on pyrrhotite in which the author is interested[18].

a) *Decrease of saturation magnetization by pressure*

It is said that the spontaneous magnetization of pyrrhotite is due to the ordered arrangement of vacancies of iron ions in crystal[2,19]. When a mechanical force is applied to this material, the decrease of the magnetization can be expected, if this force is strong enough to destroy this ordered arrangement.

The present author made an experiment of the pressure effect on pyrrhotite using the so-called Bridgemann's anvil type of squeezer[14]. According to the obtained results (Fig. 16), it can be found that the intensity of saturation magnetization decreases gradually with increasing applied pressure at room temperature, and also that the reduced magnetization thus observed by the squeezing can be restored to the original intensity by annealing at 100°C as seen in Fig. 17.

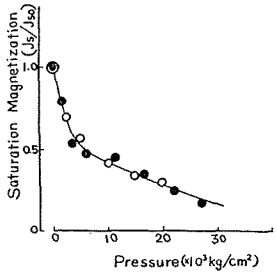

Fig. 16. Pressure dependency of the saturation magnetization of pyrrhotite. Full circles show the results for the natural specimens and hollow circles for the synthesized specimens.

This can be explained in the following way that the disordered arrangement of vacancies resulted by the application of the mechanical force is recovered by the thermal annealing to the ordered state pyrrhotite. Same tendency of the decrease of saturation magnetization has been observed when the specimen was quenched from high temperatures by Bertaut. The fact was also observed by the present author (Fig. 19).

b) *Generation of remanent magnetization by pressure*

When a one-directional pressure was applied to pyrrhotite in the geomagnetic field at room temperature, the generation of remanent magnetization which by Dōmen was called by the name piezo-remanent magnetization[20] was observed. As seen in Figs. 20 and 21, these results show that the intensity of remanent magnetization increases gradually with increasing applied pressure in the range from 700 to 20,000 kg/cm², and up to the range between 5,000 kg/cm² and 7,000 kg/cm² the inclination gradually increases, while above 7,000 kg/cm² the inclination decreases and becomes nearly perpendicular to the axis of applied pressure as shown in Fig. 21.

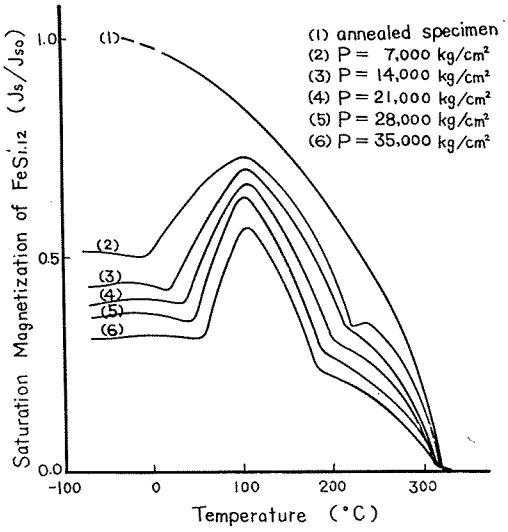

Fig. 17. Change of the intensity of the saturation magnetization of $FeS_{1.12}$ observed in a thermo-magnetic analyses after the application of one-directional pressures.

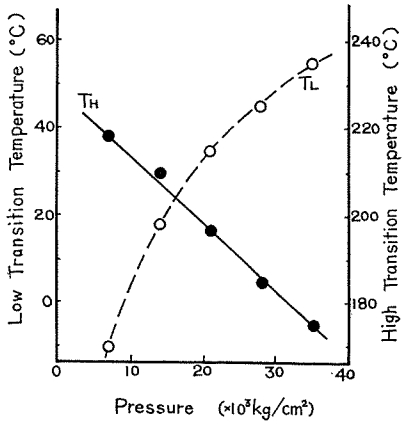

Fig. 18. Relationship between the transition temperature of $FeS_{1.12}$ and the magnitude of the applied pressure. T_H represents the high temperature transition and T_L the low temperature transition.

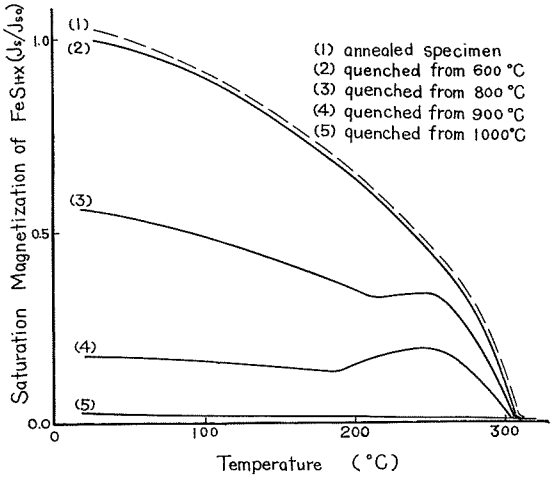

Fig. 19. Decrease of the saturation magnetization of pyrrhotite due to the quenching effect.

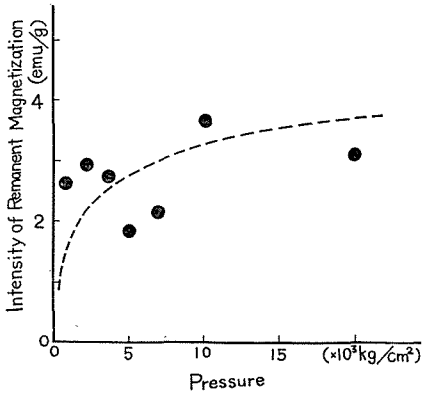

Fig. 20. Generation of piezo-remanent magnetization of pyrrhotite. The relationship between the intensity of the remanent magnetization and the magnitude of the applied pressures is shown in this diagram.

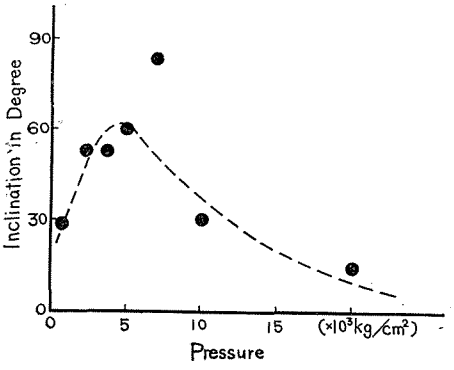

Fig. 21. Generation of piezo-remanent magnetization of pyrrhotite. The relationship between the inclination of the remanent magnetization and the magnitude of the applied pressure is shown in this diagram.

4. Interpretation available to the magnetization of Besshi Mine

In order to examine in detail the magnetization of pyrrhotite occurring in Besshi mine, it is interesting to compare the data with those obtained at Yanahara and the nature and characteristic magnetism of the synthesized pyrrhotite (Fig. 22). It is noticed that the intensity of magnetization of the former mine is weaker than that of the latter mine and also that γ-transition of the ordinary pyrrhotite to occur at 210°C[21] appears at lower temperature (about 180°C).

On the other hand, there is no noticeable difference in the magnetic properties between the pyrrhotite synthesized at high temperature in air and Yanahara's one. Geology of Yanahara Mine suggest that the formation was mainly due to a low grade hydrothermal reaction and, therefore, the condition of the formation is very close to that of the synthesized pyrrhotite. As already mentioned, the condition of formation of the ore-deposit in Besshi varies in a wider way. But it is reasonable to assume that at least some parts of the mineral have made under very high pressure, since kyanite occurrs at very ploximity of the ore-deposit. Therefore, if the effect of pressure is taken into consideration, the above-mentioned difference of the magnetic properties of the pyrrhotite at two mines may reasonably be explained, though the influence of some chemical impurities like Cu, Zn or Ni should be taken into account.

In the previous section, the present author already showed the results of the observation of the saturation magnetization of pyrrhotite at room temperature which decreases with increasing the applied pressure. Moreover, the

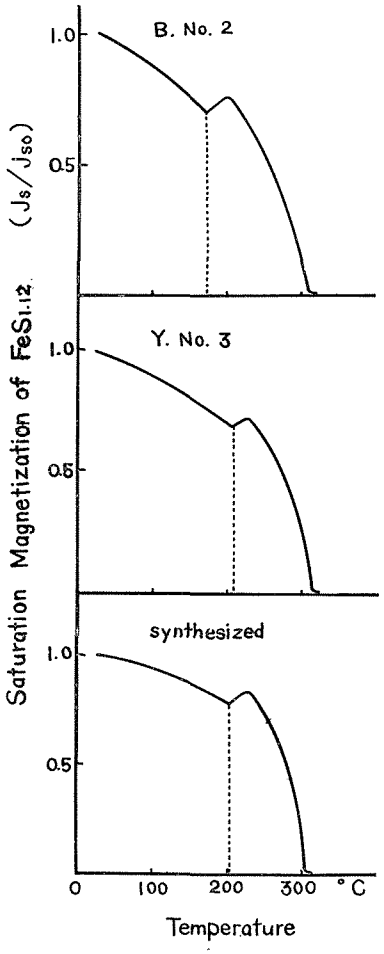

Fig. 22. Characteristic difference in thermo-magnetic curves of Besshi, Yanahara and the synthesized $FeS_{1.12}$.

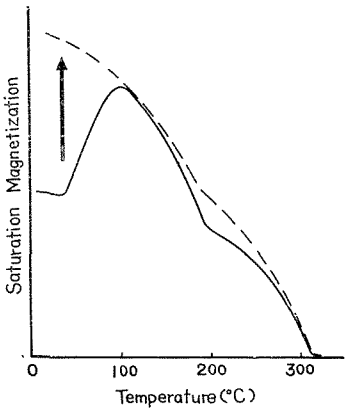

Fig. 23. Thermo-magnetic analysis of pyrrhotite from Besshi Mine. The dotted line is a curve which is expected by annealing the original mineral.

thermo-magnetic curves themselves are very much complicated indeed. For example, Fig. 17 shows that the magnetization once reduced by the application of pressure begins to recover as the temperature of the specimens is elevated, and reaches the maximum value at about 100°C. As for the knick point which should correspond to γ-transition, it can be found that the transition temperature is lowered as the applied pressures increase (Figs. 17 and 18).

Intensity of the squeezed specimens increases during heating in the thermo-magnetic analyses recovering the Bertaut's order and the ferrimagnetism as shown in Fig. 23, where the arrow shows the recovery. Whereas in the thermo-magnetic curves of Besshi pyrrhotite there appears no such recovering but lowered knick point at about 180°C. Therefore, to account for this curve the present author assumed the natural annealing in geosyncline to have taken place after the squeezing of the very mineral.

It is likely that pyrrhotite occurred from FeS_2 or $FeS \cdot nH_2O$ in the original sedimentary deposit by the applied pressure in the range from 3,500 kg/cm² to 8,000 kg/cm² as our pressure experiment of squeezing of water-containing pyrite and mixture of iron and sulfur. It is also probable that piezo-remanent

magnetism took place during the squeezing of the bed by the more or less one-directed pressure. Thus the pressure might produce host magnetic mineral of the ore-deposit and its remanent magnetism.

Some mining geologists, on the contrary, insist that pyrrhotite is the syngenetic product with the bed being made by submarine volcanic activity[22,23,24]. Regardless the mechanism of the formation of pyrrhotite and the acquisiting of the remanent magnetism, one can say that the ore-deposit has been bent in such that the lower part of the deposit is rotated relative to the upper part as the remanent vector indicate as schematically shown in Fig. 24.

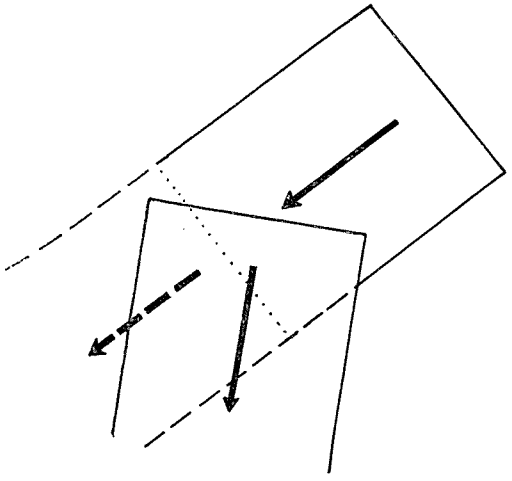

Fig. 24. Schematic diagram showing the relation between the bend of ore-deposit and the direction of magnetization in Bessh Mine. Arrows show the direction of the n.r.m..

Chapter II. Role of FeS_{1+x} on Magnetism of Rocks

1. Occurrence of pyrrhotite in sedimentary rocks

Many investigators[4,25,26] have suggested that occurrence of FeS_{1+x} covers a wide range in Japanese ingeous rocks such as gneissose mignatite and granites etc. and this mineral plays an important role on magnetization of rocks. The author reported[7,27] that FeS_{1+x} has wide occurrences in sedimentary rocks in Japan. The collecting sites of rocks containing FeS_{1+x} are shown in Fig. 1 and some results are shown in Figs. 25 and 26. Further, he discussed that pyrrhotite is an intermediate product in the removing process of pyrite to be oxidized to magnetite or haematite. Mapstone[5] also found that both of FeS_{1+x} changes into Fe_3O_4 or α-Fe_2O_3 when the oxidation proceeds. This fact suggests

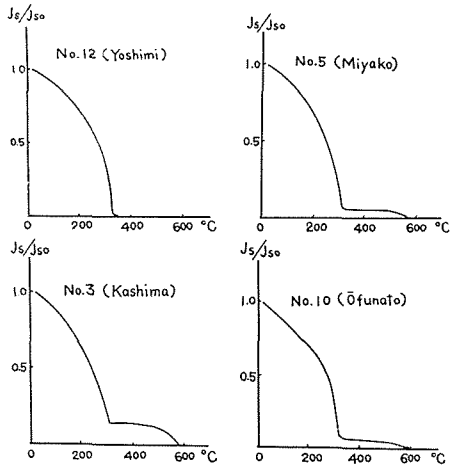

(a) black shales

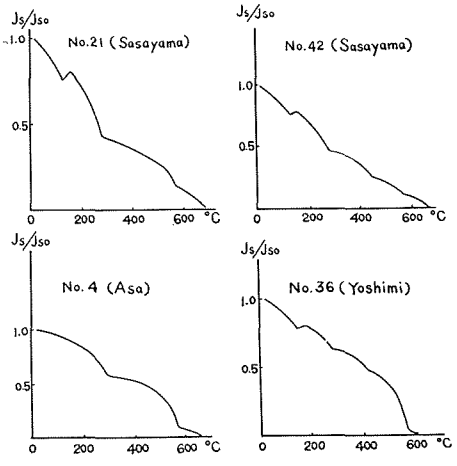

(b) red sandstones

Fig. 25. Representative examples of the thermo-magnetic curves of black shales and red sandstones.

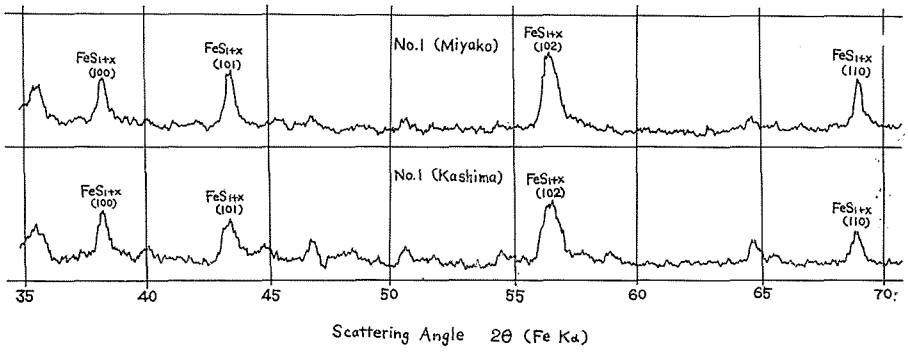

(a) black shales

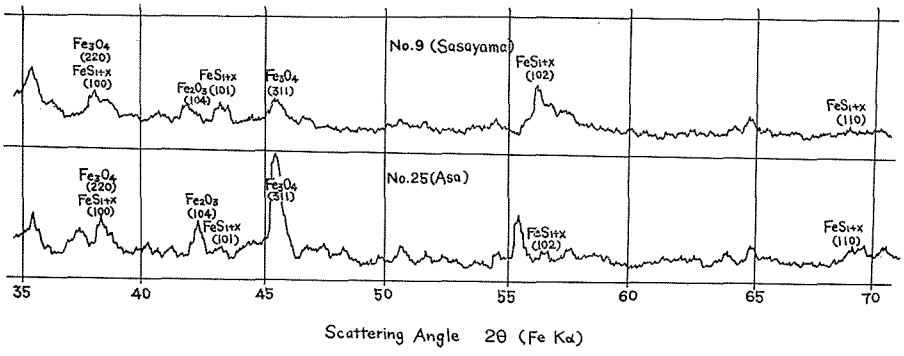

(b) red sandstones

Fig. 26. X-ray diffraction patterns of ferromagnetic minerals which were extracted from black shales and sahdstones.

that there is a possibility of the generation of chemical remanent magnetization (c.r.m.) on the process of oxidation mentioned in the above.

Consequently, several minerals are responsible to the n.r.m. of those rocks, and each one might have been magnetized by the past geomagnetic dipole field with different direction and intensity and sometimes at different geologic times. In such a case, thermal demagnetization of the n.r.m. seems to be one of the experiments by which one can clarify the process of magnetization or distinguish the original magnetization from the secondary.

2. The remanent magnetization of black and red beds

The n.r.m. of black shales and red sandstones were measured. They all are fairly strong and stable. The results are illustrated in Fig. 27 and in Table III.

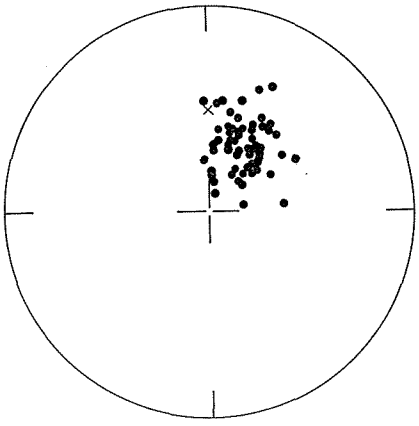

(a) Sasayama red bed

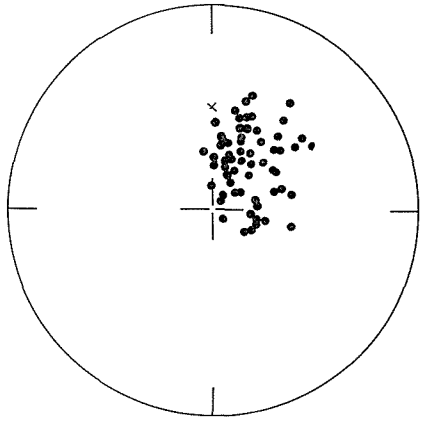

(b) Asa red bed

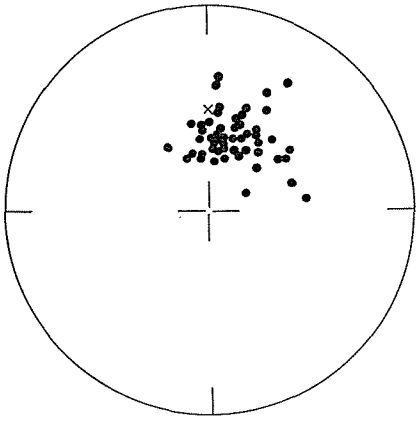

(c) Yoshimi red bed

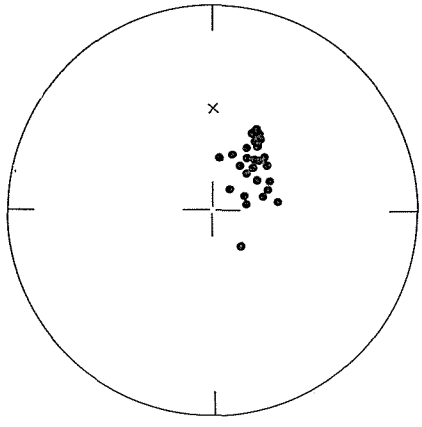

(d) Yoshimi black bed

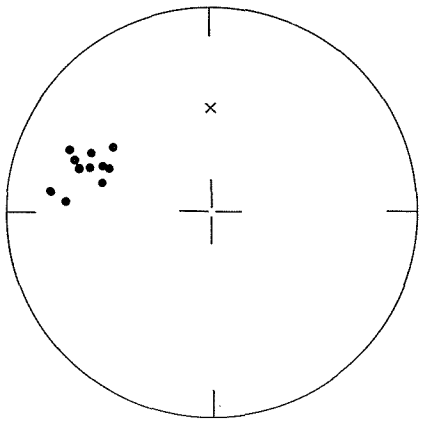

(e) Miyako black bed

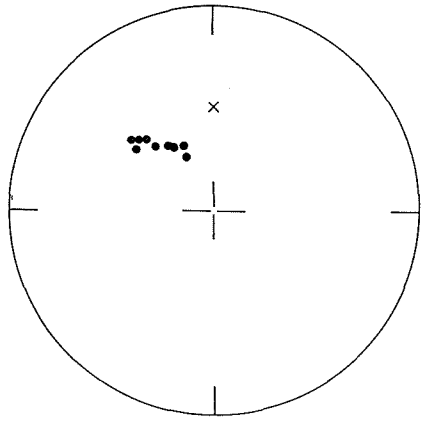

(f) Kashima black bed

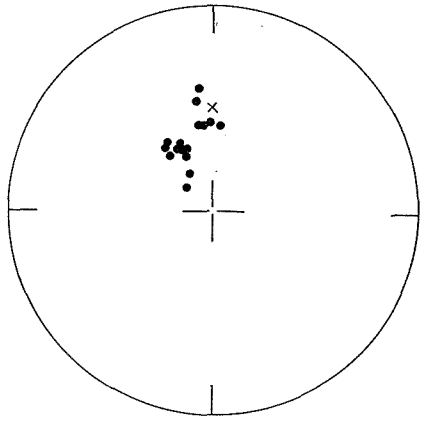

(g) Ôfunato black bed

Fig. 27. Direction of the red and black beds plotted on Schmidt's equal areal projection. Local geological dip is not corrected. × : Direction of the present dipole field.

Table III (a) Sasayama red bed

No.	Direction of Magnetization		Jr ($\times 10^{-5}$ emu/g)	Ji ($\times 10^{-6}$ emu/g)	Js ($\times 10^{-2}$ emu/g)	Ji/Jr	Jr/Js ($\times 10^{-3}$)
	Decl.	Incl.					
1	NE 42°	66°D	0.68	2.45		0.36	
2	4	74	0.80	4.32		0.54	
3	60	49	0.89	1.78	2.35	0.20	0.38
4	7	45	0.80	1.52	2.97	0.19	0.27
5	5	76	0.45	1.98		0.44	
6	17	43	0.88	0.97	1.48	0.11	0.59
7	32	57	0.85	5.78		0.68	
8	15	83	0.60	2.16		0.36	
9	10	78	1.54	4.00	1.63	0.26	0.94
10	16	55	13.10	33.70		0.26	
11	46	46	2.70	5.94	6.55	0.22	0.41
12	13	49	1.25	3.13		0.25	
13	15	57	0.32	0.58		0.18	
14	41	59	0.87	1.13		0.13	
15	46	74	0.90	2.34		0.26	
16	4	63	1.52	2.74	3.17	0.18	0.48
17	53	53	3.26	3.26		0.10	
18	81	77	3.81	3.43	6.67	0.09	0.57
19	42	64	4.92	6.40	9.33	0.13	0.53
20	37	50	4.87	12.66		0.26	
21	42	56	5.69	13.09	2.76	0.23	2.06
22	60	49	5.49	3.84	9.70	0.07	0.57
23	60	61	3.33	8.33		0.25	
24	40	57	3.46	3.70	4.02	0.11	0.86
25	29	53	4.54	20.43		0.45	
26	20	60	4.96	9.92	7.47	0.20	0.66
27	36	58	5.11	12.26	14.84	0.24	0.34
28	46	62	2.65	2.65		0.10	
29	36	59	4.26	9.37		0.22	
30	26	63	4.12	10.71	5.67	0.26	0.73
31	31	73	4.72	14.63	10.08	0.31	0.47
32	24	54	6.99	13.98		0.20	
33	51	73	2.61	3.13		0.12	
34	42	70	9.08	19.98		0.22	
35	30	46	5.95	5.36		0.09	
36	32	60	4.71	8.95	9.01	0.19	0.52
37	50	67	7.08	20.53	9.35	0.29	0.76
38	26	65	3.21	6.42		0.20	
39	36	62	3.63	2.18		0.06	
40	7	57	4.34	8.68		0.20	
41	43	61	5.27	6.32	10.64	0.12	0.50
42	21	56	4.92	7.38		0.15	
43	33	49	9.43	9.48		0.10	
44	21	57	4.14	3.73	2.71	0.09	1.53
45	16	62	3.75	5.63		0.15	
46	23	36	1.12	0.90		0.08	
47	4	65	2.49	1.24		0.05	
48	18	51	2.18	2.18		0.20	
49	13	55	1.01	2.73		0.27	
50	17	60	5.14	4.36	2.50	0.10	2.06
51	28	51	1.45	1.16		0.08	
52	7	61	1.40	1.40		0.10	
53	5	46	2.24	2.46		0.11	
54	16	62	4.54	27.24	17.50	0.60	0.26
55	− 5	69	7.80	33.54	47.58	0.43	0.16
56	50	65	2.24	1.34		0.06	
57	33	70	1.70	10.88		0.64	
Mean	28	61	3.54	7.37	8.54	0.22	0.71
Error	3.0		1.98	5.45	3.59	0.11	0.37

(b) Asa red bed

No.	Direction of Magnetization		Jr ($\times 10^{-5}$ emu/g)	Ji ($\times 10^{-6}$ emu/g)	Js ($\times 10^{-2}$ emu/g)	Ji/Jr	Jr/Js ($\times 10^{-3}$)
	Decl.	Incl.					
1	NE102°	72°D	2.59	1.30		0.05	
2	102	69	1.89	3.21		0.17	
3	108	72	0.85	1.79		0.21	
4	80	73	1.28	0.77	2.31	0.06	0.55
5	118	72	1.99	1.59	1.40	0.08	1.42
6	58	61	1.97	1.18		0.06	
7	121	63	2.31	1.85		0.08	
8	124	74	1.68	1.85		0.11	
9	86	72	1.65	2.81		0.17	
10	96	74	5.50	7.70	3.37	0.14	1.63
11	102	57	3.93	0.39	1.64	0.01	2.40
12	49	54	1.49	2.38	1.68	0.16	0.89
13	52	48	2.18	2.83		0.13	
14	37	36	0.68	1.56		0.23	
15	60	61	2.14	3.00	2.72	0.14	0.79
16	52	44	2.62	3.67		0.14	
17	48	62	4.91	4.42		0.09	
18	41	66	3.61	4.69		0.13	
19	13	49	3.82	8.02		0.21	
20	17	44	7.16	13.10	7.81	0.19	0.92
21	21	50	4.57	11.88		0.26	
22	16	51	4.42	6.19		0.14	
23	1	55	4.84	15.30		0.31	
24	23	50	4.01	4.01		0.10	
25	19	41	5.01	17.03	24.88	0.34	0.20
26	9	62	2.65	3.18		0.12	
27	18	55	4.73	17.97		0.38	
28	23	55	3.85	11.55	11.82	0.30	0.33
29	35	57	3.37	2.36	0.83	0.07	4.06
30	43	51	4.87	6.82		0.14	
31	35	63	2.32	3.94		0.17	
32	58	42	3.06	3.98		0.13	
33	39	44	5.95	13.09		0.22	
34	47	56	2.34	4.46		0.19	
35	28	73	1.80	1.98	1.50	0.11	1.20
36	16	73	0.78	7.02		0.09	
37	9	67	0.93	2.05	0.95	0.22	0.98
38	7	64	3.25	5.20		0.16	
39	37	83	2.03	2.23		0.11	
40	0	69	2.39	0.24		0.01	
41	11	63	2.29	1.60		0.07	
42	15	70	2.22	3.14		0.14	
43	20	69	2.56	2.30		0.09	
44	16	68	1.85	0.56	0.85	0.03	2.18
45	7	61	1.59	2.39		0.15	
46	25	64	0.64	0.64		0.10	
47	21	60	0.45	0.95	1.19	0.21	0.38
48	0	80	2.14	3.64		0.17	
49	34	77	1.91	3.82		0.20	
50	60	77	0.72	3.02		0.42	
51	80	58	1.03	2.58		0.25	
52	2	73	1.31	1.44	1.60	0.11	0.82
53	43	85	1.40	1.54		0.11	
54	53	79	0.24	0.38		0.16	
55	131	84	1.71	3.25	1.70	0.19	1.01
Mean	39	66	2.61	4.34	4.14	0.16	1.61
Error	4.4		1.07	3.07	3.97	0.06	0.85

(c) Yoshimi red bed

No.	Direction of Magnetization		Jr ($\times 10^{-5}$ emu/g)	Ji ($\times 10^{-6}$ emu/g)	Js ($\times 10^{-2}$ emu/g)	Ji/Jr	Jr/Js ($10\times^{-3}$)
	Decl.	Incl.					
1	NE 72°	54°D	4.36	12.90		0.30	
2	55	50	2.05	2.46		0.12	
3	41	52	5.19	18.16		0.35	
4	47	65	5.83	18.07	1.20	0.31	4.86
5	54	56	4.36	13.95		0.32	
6	18	55	5.11	12.88		0.25	
7	29	43	5.51	11.02	16.96	0.20	0.32
8	19	66	1.44	1.87		0.13	
9	29	52	4.64	12.64		0.26	
10	20	46	3.24	3.89		0.12	
11	− 4	55	1.24	2.36		0.19	
12	− 6	60	1.51	0.91		0.06	
13	7	70	2.24	6.72		0.30	
14	− 6	67	7.91	31.64	2.42	0.40	3.27
15	12	60	2.79	18.69		0.67	
16	6	50	2.80	7.28		0.26	
17	−21	67	1.49	2.38		0.16	
18	− 6	68	1.82	9.10		0.50	
19	19	49	3.27	18.97		0.58	
20	65	74	2.31	9.12		0.36	
21	32	53	2.23	7.81	175.67	0.35	0.01
22	23	63	3.12	8.74		0.28	
23	−15	66	1.10	0.99		0.09	
24	9	66	1.20	0.96		0.08	
25	40	59	9.21	57.68	76.09	0.80	0.12
26	17	68	3.39	18.31		0.54	
27	8	57	7.05	26.79		0.38	
28	37	55	7.00	16.10	28.68	0.23	0.24
29	0	54	5.88	12.91		0.24	
30	14	64	4.34	9.98		0.23	
31	56	53	4.43	13.81		0.31	
32	28	65	3.17	6.97		0.22	
33	−11	54	5.22	19.31		0.37	
34	36	56	3.56	19.88		0.47	
35	6	63	3.96	11.88		0.30	
36	3	60	6.29	19.50	32.32	0.31	0.19
37	9	61	6.45	36.12		0.56	
38	17	51	5.44	17.41		0.32	
39	7	60	5.81	17.43		0.30	
40	6	65	8.18	40.90	43.26	0.50	0.19
41	− 5	58	7.42	23.00		0.31	
42	7	59	7.03	15.47		0.22	
43	6	48	7.91	25.31		0.32	
44	20	53	7.80	33.54		0.43	
45	13	63	7.37	22.85	62.50	0.31	0.12
Mean	18	58	4.53	15.52	48.80	0.32	1.04
Error	1.5		1.92	8.41	37.31	0.11	1.35

(d) Yoshimi black bed

No.	Direction of Magnetization		Jr ($\times 10^{-5}\frac{emu}{g}$)	Ji ($\times 10^{-6}\frac{emu}{g}$)	Js ($\times 10^{-2}\frac{emu}{g}$)	Ji/Jr	Jr/Js ($\times 10^{-3}$)
	Decl.	Incl.					
1	NE 31°	65°D	2.39	4.54		0.19	
2	63	64	28.37	42.56	4.85	0.15	5.85
3	70	66	16.85	26.96	5.77	0.16	2.92
4	82	64	2.19	1.75		0.08	
5	75	69	3.56	3.92		0.11	
6	53	69	2.05	2.46		0.12	
7	19	66	3.47	5.55		0.16	
8	65	76	34.62	48.47	3.49	0.14	9.92
9	79	76	51.03	51.03		0.01	
10	73	70	33.39	31.07		0.08	
11	34	69	28.33	23.21		0.07	
12	44	60	31.75	19.05	13.40	0.06	2.37
13	43	66	19.69	3.94		0.02	
14	34	58	29.88	32.87		0.11	
15	42	63	4.25	1.28		0.03	
16	33	55	32.64	39.17	2.02	0.12	16.16
17	28	53	19.65	13.76		0.07	
18	27	54	10.50	12.60		0.12	
19	43	70	27.37	24.63	1.14	0.09	24.01
20	30	54	21.08	14.76		0.07	
21	50	62	1.27	0.51		0.04	
22	32	57	0.57	0.85		0.15	
23	6	69	0.86	0.53		0.07	
24	39	63	0.75	0.23		0.03	
Mean	4.5	64	16.94	16.90	5.11	0.10	10.21
Error	4.5		12.88	13.80	2.98	0.04	6.59

(e) Miyako black bed

No.	Direction of Magnetization		Jr ($\times 10^{-5}\frac{emu}{g}$)	Ji ($\times 10^{-6}\frac{emu}{g}$)	Js ($\times 10^{-2}\frac{emu}{g}$)	Ji/Jr	Jr/Js ($\times 10^{-3}$)
	Decl.	Incl.					
1	NW71°	32°D	12.60				
2	63	35	6.28		3.69		1.70
3	75	44	5.88				
4	82	22	7.24				
5	66	44	6.47		6.52		0.99
6	66	25	1.12				
7	68	29	3.55				
8	85	29	2.83	3.83	2.29	0.14	1.24
9	56	42	10.00	7.03		0.07	
10	66	42	25.40				
11	69	36	25.40	1.35	3.85	0.01	6.60
Mean	70	35	9.71	4.07	4.17	0.25	2.66
Error	5.9		6.29	1.95	1.57	0.18	2.00

(f) Kashima black bed

No.	Direction of Magnetization		Jr $(\times 10^{-5}\frac{emu}{g})$	Ji $(\times 10^{-6}\frac{emu}{g})$	Js $(\times 10^{-2}\frac{emu}{g})$	Ji/Jr	Jr/Js $(\times 10^{-3})$
	Decl.	Incl.					
1	NW43°	50°D	5.34		1.67		3.20
2	35	58	12.70				
3	32	60	7.13		8.78		0.81
4	24	61	1.29				
5	46	48	5.08				
6	51	50	3.20				
7	27	66	0.92				
8	49	46	2.60				
9	42	55	3.80				
Mean	40	55	4.67		5.23		2.01
Error	5.5		2.57		3.55		1.20

(g) Ôfunato black bed

No.	Direction of Magnetization		Jr $(\times 10^{-4}\frac{emu}{g})$	Ji $(\times 10^{-5}\frac{emu}{g})$	Js $(\times 10^{-2}\frac{emu}{g})$	Ji/Jr	Jr/Js $(\times 10^{-3})$
	Decl.	Incl.					
1	NW 8°	54°D	2.68	2.04		0.08	
2	6	45	3.81	3.63		0.09	
3	2	55	3.27	3.54		0.11	
4	5	55	2.96				
5	9	55	2.00				
6	6	40	4.24	2.04	4.77	0.05	8.89
7	48	76	0.28				
8	31	72	0.41				
9	26	62	1.54				
10	28	62	0.32	0.21	9.89	0.07	0.32
11	22	63	2.01		12.80		1.57
12	37	62	1.42				
13	33	57	1.69				
14	36	58	1.78				
15	25	65	0.16				
16	25	60	0.14	0.51	14.90	0.36	0.01
Mean	19	59	1.80	1.99	10.59	0.13	2.70
Error	5.2		1.08	1.09	3.01	0.08	2.85

Fig. 28 is also the results of the measurements of the n.r.m. in which the corrections for the strata are made. As seen in the figure, the results becomes more scattered when the correction was made, suggesting that the so-called secondary magnetization took place after the folding of the sedimentary beds.

3. Thermal demagnetization of rocks

As was previously stated, Japanese sedimentary rocks occasionally contain FeS_{1+x}, Fe_3O_4 and α-Fe_2O_3. And it was put into a qusetion whether or not the time of those magnetization is later than the formation of the beds. If the existence of intermediate state from FeS_{1+x} to other iron oxides can be considered due to a certain chemical reaction through geologic time, the

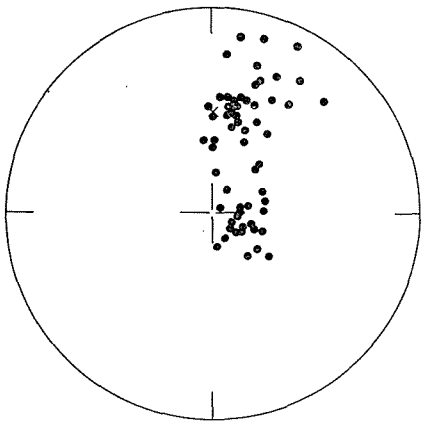

(a) Sasayama red bed

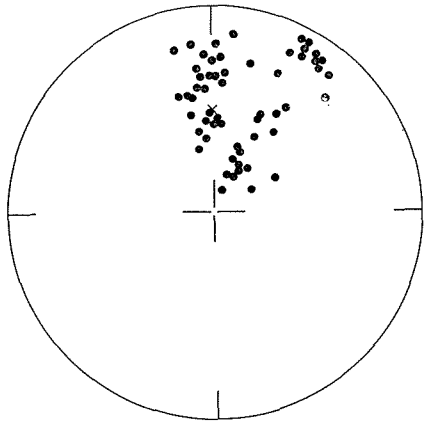

(b) Asa red bed

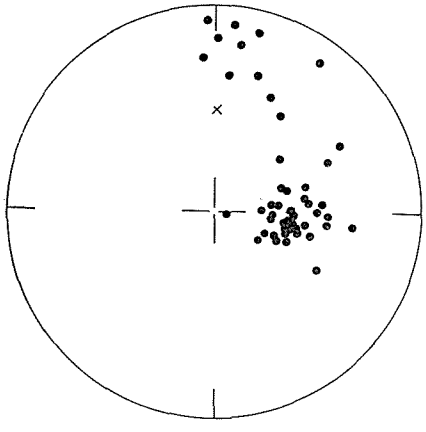

(c) Yoshimi red bed

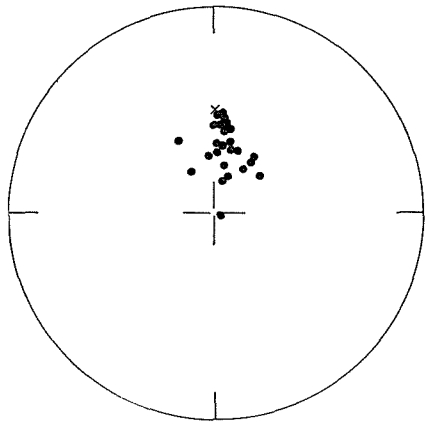

(d) Yoshimi black bed

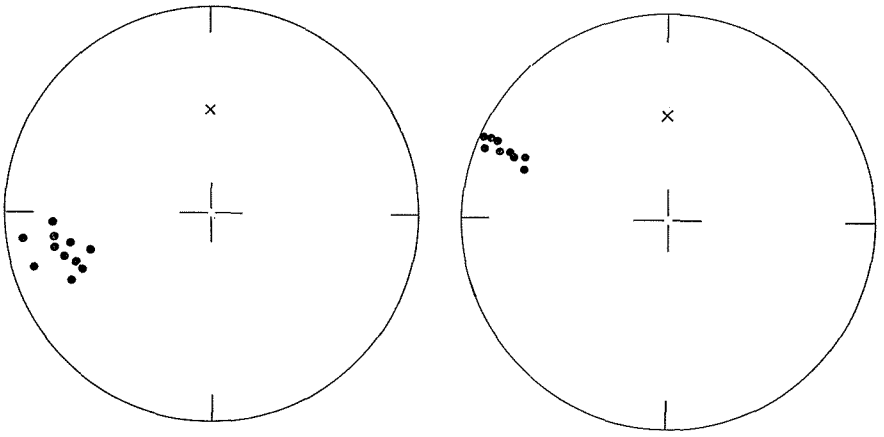

(e) Miyako black bed (f) Kashima black bed

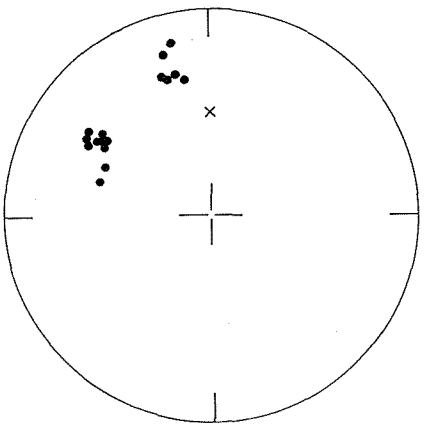

(g) Ôfunato black bed

Fig. 28. *Direction of the n.r.m. of the red and black beds plotted on Schmidt's equal areal projection. Local geological dip is corrected.* × : Direction of the present dipole field.

direction of remanent magnetization measured should be that of the resultant remanent vectors, some being acquired at certain geologic time and some in the other. Therefore, it is necessary to distinguish one from the other by demagnetization of rocks. Of which thermal demagnetization is useful, since FeS_{1+x}, Fe_3O_4 and α-Fe_2O_3 have different Curie points in the order of increasing temperature, and, therefore, by heating and measuring at each Curie point one can seperate the vector due to each ferromagnetic phase.

First, the samples were cut off into cube of the size of (3.3 cm^3), and were rotated inside a quartz furnace put under the astatic magnetometer. To make the furnace, a quartz tube of 6.5 cm in diameter and 70 cm in length was prepared, and platinum wire of 0.5 mm in diameter and 10 m in length was wound non-magnetically in such that the number of turns are greater at the end of the tube and smaller in the center so that the temperature inside may be as uniform as possible. The tube was enclosed with quartz wool and quartz tape as thermal insulators. In this non-magnetic furnace, by rotating the sample with a specially equipped sample holder three components of the magnetization of rocks were measured at appropriate temperature. A schematic diagram of this apparatus is in Fig. 29.

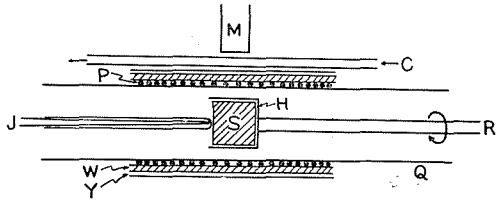

Fig. 29. Schematic diagram of thermo-demagnetizing apparatus. M: astatic magnetometer, C: water cooler, P: platinum wire heater (non-inductively wound), H: sample holder, S: sample, J: thermo-junction, R: rotating rod, Q: quartz tube, W: quartz wool, Y: quartz tape.

69 samples whose remanent magnetization was already observed at room temperature were selected and each change of the magnetization with increasing temperature was examined. Some of the curves thus obtained are shown in Fig. 30. As already examined, Curie point of FeS_{1+x} is about 300°C above which the component vector due to this phase disappears and, therefore, the remanence to be due to the phase having higher Curie point, for example to Fe_3O_4 or α-Fe_2O_3. By subtracting the remanent vector at 300°C from original vector, one can find the component vector due to FeS_{1+x}. When the similar procedure is carried out at 575°C remanent vector due to magnetite or haematite is to be seperated.

However, the measurement above 580°C was practically impossible. Table IV shows the results thus obtained. In those results, the correction for the tilt of the strata was made. Individual errors of measurement of each rock sample were fairly large, however, if we take mean direction of component vector due to pyrrhotite and the other, they all differ from each other as shown in Fig. 31. For example, both in the black bed and in the red bed the remanent magnetization due to FeS_{1+x} differs slightly from that due to other iron oxides.

As shown in Fig. 30 and Table IV the remanent magnetization of black shale depends mainly on FeS_{1+x} and partly on Fe_3O_4, the rate of dependency

being about 70 : 30 in average, while that of red sandstones depends on FeS_{1+x}, Fe_3O_4 and α-Fe_2O_3, the rate being about 35 : 45 : 20 respectively in average.

Accordingly, one can say that the ferromagnetism of FeS_{1+x} is not only of great importance in black beds, but also plays a fairly important role even in red beds.

Table IV

(a) Sasayama red bed

No.	Direction of Magnetization						Intensity-ratio of Magnetization	
	Jr		Jr′		Jr″		Jr′/Jr	Jr″/Jr
	Decl.	Incl.	Decl.	Incl.	Decl.	Incl.		
19	NE 11°	56° D	NE 18°	48° D	NE −2°	64° D	0.51	0.49
20	18	42	23	27	14	52	0.35	0.65
21	10	46	−16	40	45	44	0.48	0.52
22	23	42	16	30	29	51	0.44	0.56
23	26	58	−27	56	48	51	0.38	0.62
24	15	49	−3	50	27	53	0.50	0.50
25	10	43	−19	43	40	35	0.49	0.51
29	11	49	32	68	4	37	0.36	0.64
31	−6	60	10	51	−29	67	0.42	0.58
33	3	64	26	54	−37	69	0.45	0.55
34	4	60	−16	70	14	50	0.45	0.55
36	104	75	119	68	20	75	0.64	0.36
36′	112	76	137	74	71	71	0.65	0.35
38	122	78	−173	72	82	69	0.51	0.49
40	51	85	−129	59	67	42	0.30	0.70
42	78	79	100	72	0	80	0.71	0.39
43	74	68	100	52	3	70	0.44	0.56
45	109	82	65	77	161	80	0.44	0.56
47	154	79	32	79	170	65	0.35	0.65
49	94	80	144	84	69	68	0.58	0.42
50	115	78	109	43	−163	85	0.20	0.80
55	178	85	−71	70	125	66	0.40	0.60
Mean I	NE 12°	52° D	NE 4°	50° D	NE 20°	55° D	0.46	0.54
Mean II	NE 104°	80° D	NE 122°	78° D	NE 78°	79° D		

I: Mean values of Jr, Jr′, and Jr″ of rocks collected from north dipping strata.
II: Mean values of Jr, Jr′ and Jr″ of rocks collected from south dipping strata.
Jr: The n.r.m. measured at room temperature, Jr′: The magnetic moment disappeared by heating to 330°C, Jr″: The remanent magnetic moment at 330°C.

(b) Asa red bed

No.	Direction of Magnetization						Intensity-ratio of Magnetization	
	Jr		Jr′		Jr″		Jr′/Jr	Jr″/Jr
	Decl.	Incl.	Decl.	Incl.	Decl.	Incl.		
I	NE 28°	70° D	NE 17°	22° D	NE 42°	78° D	0.13	0.87
2′	−3	59	21	31	−13	64	0.22	0.78
8	21	75	−34	38	60	76	0.18	0.82
9	23	64	25	53	23	77	0.56	0.44
16	35	38	24	41	44	36	0.46	0.54
17	7	52	8	52	−2	55	0.65	0.35
18	−2	51	4	39	−20	71	0.37	0.63
19	−4	30	−21	36	8	26	0.46	0.54
22	−2	32	25	58	−16	12	0.35	0.65
24	3	33	−1	32	8	44	0.70	0.30
25′	−24	40	−40	46	−19	39	0.35	0.65
26′	−14	30	−20	11	−13	44	0.26	0.74
27	−4	36	7	30	−26	54	0.40	0.60
31	−15	24	1	32	−20	20	0.30	0.70
32	15	27	36	31	−5	20	0.38	0.62
34	−2	26	5	31	−9	29	0.35	0.65
Mean	NE 2°	44° D	NE 1°	38° D	NE 4°	49° D	0.38	0.62

(c) Yoshimi red bed

No.	Direction of Magnetization						Intensity-ratio of Magnetization	
	Jr		Jr′		Jr″		Jr′/Jr	Jr″/Jr
	Decl.	Incl.	Decl.	Incl.	Decl.	Incl.		
11	NE 80°	67° D	NE 106°	72° D	NE 66°	58° D	0.32	0.68
12	92	68	61	69	40	66	0.10	0.90
19	73	53	52	87	81	22	0.32	0.68
26	108	55	104	65	113	42	0.47	0.53
27	89	60	86	56	80	53	0.00	1.00
28	90	45	59	36	123	49	0.39	0.61
28′	111	56	109	43	114	65	0.33	0.67
34	92	46	23	83	96	30	0.14	0.86
35′	94	41	75	43	104	40	0.22	0.78
37	97	59	133	55	72	54	0.35	0.65
39′	39	74	42	64	−144	88	0.44	0.56
40	104	61	52	52	121	58	0.17	0.83
41	91	61	126	62	70	57	0.38	0.62
45	100	57	90	51	121	61	0.37	0.63
Mean	NE 92°	58° D	NE 84°	63° D	NE 94°	55 °D	0.29	0.71

(d) Yoshimi black bed

No.	Direction of Magnetization						Intensity-ratio of Magnetization	
	Jr		Jr′		Jr″		Jr′/Jr	Jr″/Jr
	Decl.	Incl.	Decl.	Incl.	Decl.	Incl.		
2′	NE 32°	62° D	NE 32°	54° D	NE 28°	72° D	0.54	0.46
4	49	66	53	60	−4	79	0.65	0.35
6	19	63	90	82	5	20	0.80	0.20
7	0	55	5	64	−24	44	0.58	0.42
12	12	61	17	59	−14	66	0.59	0.41
15	6	64	13	65	−26	31	0.89	0.11
16	8	54	13	52	−13	59	0.68	0.32
18	4	51	5	51	−10	57	0.83	0.17
19	−5	68	0	68	−25	65	0.86	0.14
21	14	65	26	76	9	51	0.50	0.50
22′	45	55	40	54	151	67	0.76	0.24
Mean	NE 17°	61° D	NE 31°	62° D	NE 7°	60° D	0.70	0.30

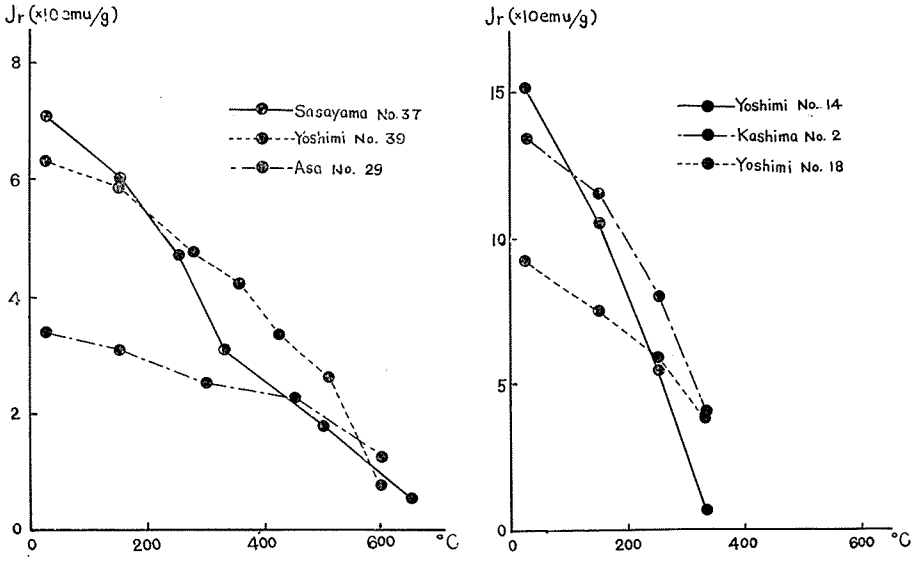

(a) red sandstones (b) black shales

Fig. 30. Temperature dependencies of remanent magnetizatian of red sandstones and black shales.

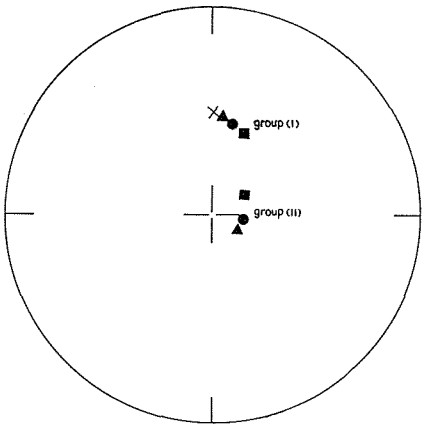

(a) Sasayama red bed

Group (I) is the results obtained from the north-dipping stratum, and group (II) from the south-dipping stratum.

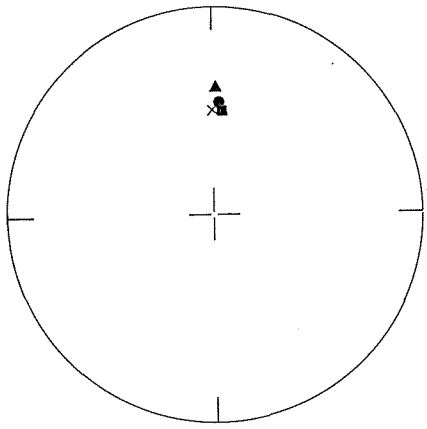

(b) Asa red bed

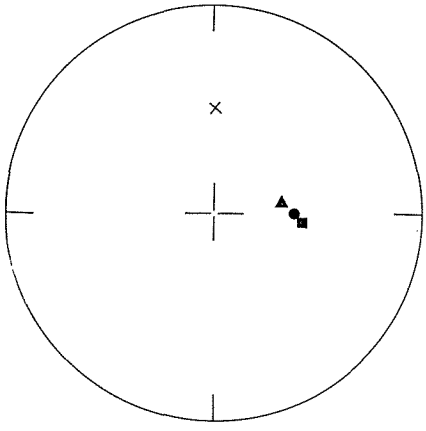

(c) Yoshimi red bed

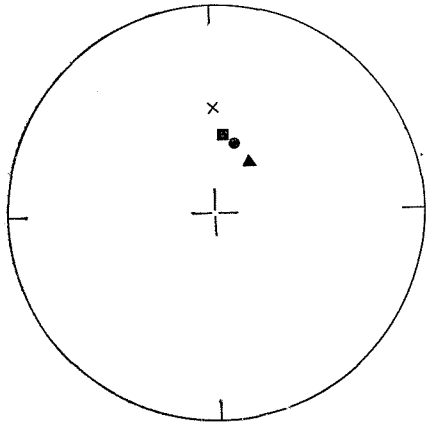

(d) Yoshimi black bed

Fig. 31. Relation of the mean direction of the n.r.m. to the magnetization due to pyrrhotite and other ferromagnetic minerals contained in same rocks. × : direction of the present geomagnetic field (H), ● : direction of the n.r.m. (Jr), ▲ : direction of magnetization due to pyrrhotite (Jr′), ■ : direction of magnetization due to magnetite and haematite (Jr″)

4. Consideration on the magnetization of rocks

According to the present author's investigations, it was confirmed that the red and black beds generally contain pyrrhotite with other iron oxides such as Fe_3O_4 and α-Fe_2O_3 as well as in the iron-sulfide mines and they possess fairly strong and stable remanent magnetizations which are to be considered as a fossil geomagnetism of the past geomagnetic dipole field. It is generally accepted in geologists that the black bed is a product of marine or lacustrine deposition under a warm and damp climate where biochemical reaction may take place in favour of its formation[28),29)], while the origin of Japanese red bed in generally associated with volcanic activities[30)].

Some important facts were suggested from the previously obtained results. Of which the one is that in the red sandstones the deviation of the remanent vector due to FeS_{1+x} from that of the present geomagnetic dipole field is smaller as compared with those due to other iron oxides, whereas in the black shales the deviation is greater than due to the latter.

It is presumed that the coexistence of pyrrhotite with other iron oxides is due to oxidation of iron sulfides such as markasite, pyrrhotite, melnikovite and hydrotroilite deposited and stratified in marine by some submarine volcanic activities or by some biochemical procedures etc.[31)]. The results obtained by thermal demagnetization of Yoshimi's black bed suggest that the above presumption is very plausible; that is to say, a chemical change from iron sulfides to iron oxides actually took place very slowly through the geological time and a chemical remanent magnetization (c.r.m.) should be taken into consideration to the magnetization of black bed. On the other hand, the results obtained from the red beds, typical one of them being Sasayama red bed, differ distinctly from those of the black bed.

The results of thermal demagnetization of Sasayama red sandstones are summarized in Fig. 31 (a), where two groups of plots are seen, each group consisting of one circle, triangle and square. Of these symbols, circles represent the mean direction of the remenent magnetization of pyrrhotite and squares that of ferromagnetic minerals with the Curie points higher than 330°C (they are proved to be magnetite and haematite by X-ray and thermo-magnetic analyses). The group (I) in the diagram illustrates the results of rocks collected from north-dipping stratum and the group (II) illustrates that from south-dipping stratum. The local dips of the strata have been corrected. As seen in the diagram, the direction of magnetization due to pyrrhotite (Jr′) of group (I) situates on the same side of the present dipole field (H) from that of the n.r.m. (Jr). In group (II), however, (Jr′) situates on the opposite side of (H) from (Jr). The magnetization due to magnetite and haematite shows the opposite situation, that is, it is on the opposite side of (H) from (Jr) in group (I) and on the same side of (H) from (Jr) in group (II).

To explain these facts, a schematic diagram is drawn in Fig. 32. In this diagram, it is assumed that pyrrhotite has been magnetized after the bend of

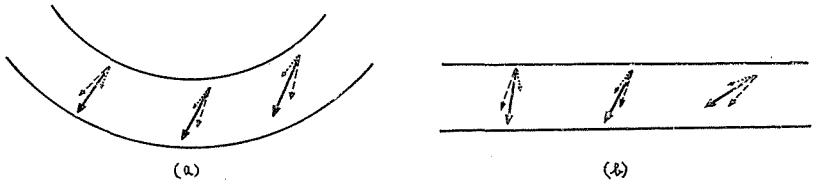

Fig. 32. Configuration of remanent magnetization of Sasayama red bed in relation to the bending of stratum. —— Jr: natural remanent magnetization, ·····Jr′: magnetic moment disappeared at 330°C (magnetization due to FeS_{1+x}), ——Jr″: remanent magnetic moment at 330°C (magnetization due to Fe_3O_4 and α-Fe_2O_3). (a) Direction of remanent magnetization of the bed, whose local dip is not corrected, (b) Direction of remanent magnetization of the bed, whose local dip is corrected.

strata took place, the direction of magnetization in north-dipping strata being nearly parallel to that in south-dipping strata if we do not correct the local dip and, it is also assumed that magnetite and haematite had been magnetized before the bend of strata happened and naturally the direction of magnetization of these minerals in north-dipping strata is parallel to that in south-dipping strata when the correction of the local dip is made. Consequently, when the dip of strata is corrected, the direction of magnetization due to pyrrhotite becomes shallower in north-dipping sites and becomes deeper in south-dipping sites. When the dip of strata is not corrected, the magnetization due to magnetite and haematite in north-dipping strata becomes deeper compared with that in south-dipping strata. This idea is merely a simple hypothesis and does not show a perfect agreement with the experimental fact but still suggests that nearly the same sort of the mechanism of magnetization as this assumption had proceeded in nature. It is needless to say that actual process of magnetization has been more complicated and it is likely that two kinds of magnetite and haematite are contained in one rock, one being original minerals which had existed at the time of formation of rocks and the other being secondary minerals produced by oxidation process represented as follows:

pyrite → pyrrhotite → magnetite → haematite

In this case, the magnetization of the primary magnetite and haematite should differ from that the secondary ones. If it were possible to distinguish the former from the latter and if we could discuss the magnetization due to primarily existed magnetite and haematite, the above-stated hypothesis could more useful to explain the experimental results.

Therefore, what the present writer can summarize his data at present is that in red beds the remanent magnetic vector due to iron oxides is more important to the palaeomagnetic investigations than those due to pyrrhotite and vice versa in black beds.

Acknowledgments

The present author devotes his hearty thanks to Dr. N. KAWAI, under whose guidances the study has been carried out.

The author's gratitudes are also expressed to Emeritus Professor N. KUMAGAI, Professor Z. HATSUDA, Professor S. MATSUSHITA and Dr. Y. NAKAMURA for their encouragements and advices given to him.

The acknowledgments are also to Professor H. YOSHIZAWA and Dr. T. TAKADA, under whose direction the microscopic observations and X-ray analyses have been made. The author also thanks to Mr. H. ITO for the kind offer of his rock collection and also his help on measuring the thermal demagnetization of rocks and also to Dr. M. KIYAMA who helped him for the synthesis work under high temperature.

References

1) NICHOLLS, G. D.: Adv, Phys., **4**, 164, 1955.
2) NÉEL, L.: Rev. Mod. Phys., **25**, 61, 1953.
3) HARALDSEN, H.: Zeit. Anorg. Allg. Chem., **231**, 78, 1939.
4) SASAJIMA, S.: Mem. Fac. Lib. Art., Fukui Univ., Ser. 2, Nat. Sci., No. 10, 147, 1960 (in Japanese).
5) ERD, R. C., EVANS, H. T., Jr. and RICHTER, D. H.: J. Min. Soc. Ame., **42**, 309, 1957.
6) HAYASE, K. and HARADA, T.: Nippon Kogyo-Kaishi, **68**, 513, 1952 (in Japanese).
7) KAWAI, N. and KANG, Y.: *Mem. Coll. Sci., Univ. Kyoto*, Ser. B, **28**, 285, 1961.
8) KAWAI, N.: J. Geophys. Res., **56**, 73, 1951.
9) YUN, I.: Mem. Coll. Sci., Univ. Kyoto, Ser. B, **25**, 125, 1958.
10) KATO, T.: J. Geol. Soc. Jap., **1**, 77, 1924.
11) UEDA, A.: Busseiron Kenkyu, **33**, 55, 1950 (in Japanese).
12) NISHIHARA, K. and KONDO, Y.: Mem. Fac. Engin., Univ. Kyoto, **20**, 285, 1958.
13) HAYASE, K. and HARADA, T.: Nippon Kogyo-Kaishi, **73**, 486, 1957 (in Japanese).
14) KAWAI, N.: J. Geomag. Geoelec., **9**, 140, 1957.
15) YASUKAWA, K.: *Mem. Coll. Sci., Univ. Kyoto*, Ser. B, **26**, 225, 1959.
16) KAWAI, N., ITO, H., YASUKAWA, K. and KUME, S.: Mem. Coll. Sci., Univ. Kyoto, Ser. B, **26**, 237, 1959.
17) DÔMEN, H.: Bull. Fac. Edu., Yamaguchi Univ., **10**, 71, 1961.
18) YUZURI, M., KANG, Y. and GOTO, Y.: "Reduction of Saturation Magnetization by Quenching and Pressure Squeezing in Some Ferrimagnetic Compounds" lectured at International Conference of Magnetism and Crystallography, 1961 (in press).
19) BERTAUT, F.: Acta. Cryst., **6**, 557, 1953.
20) DÔMEN, H.: Bull. Fac. Edu., Yamaguchi Univ., **41**, 1958.
21) TSUYA, N., TSUBOKAWA, I. and YUZURI, M.: Metal Phys., **4**, 140, 1958 (in Japanese).
22) KOJIMA, G. and HIDE, K.: J. Sci.. Hiroshima Univ., Ser. C, **2**, 195, 1958.
23) HIDE, K.: Geol. Rep., Hiroshima Univ., 9, 27, 1961 (in Japanese).
24) WATANABE, T.: "Progress in Mining Geology", Toyama, Tokyo, 438, 1961 (in Japanese).
25) HIROTA, S.: Geol. Soc. Jap., **66**, 517, 1960 (in Japanese).
26) OKAMURA, Y.: J. Geol. Soc. Jap., **63**, 684, 1957 (in Japanese).

27) KAWAI, N. and KANG, Y.: "Magnetism of Black Shale and Red Sandstone in Japan" lectured at Special Meeting on Rock Magnetism in International Conference of Magnetism and Crystallography, 1961 (in press).
28) TWENHOFEL, W. H.: "Principle of Sedimentation", McGraw-Hill, New York and London, 396, 1939.
29) PETTIJOHN, F. J.: "Sedimentary Rocks", Harper, New York, 624, 1957.
30) KOBAYASHI, T.: "Chūgoku District", Asakura, Tokyo, 1950 (in Japanese).
31) WATANABE, T.: J. Soc. Min. Geol., 7, 87, 1957 (in Japanese).